A&A 401, 161–172 (2003)
DOI: 10.1051/0004-6361:20030118

Astronomy & Astrophysics

Intraday variability in compact extragalactic radio sources

II. Observations with the Effelsberg 100 m radio telescope

A. Kraus[1], T. P. Krichbaum[1], R. Wegner[1], A. Witzel[1], G. Cimò[1], A. Quirrenbach[2], S. Britzen[1,⋆], L. Fuhrmann[1], A. P. Lobanov[1], C. E. Naundorf[1], K. Otterbein[1], B. Peng[1,3], M. Risse[1], E. Ros[1], and J. A. Zensus[1]

[1] Max-Planck-Institut für Radioastronomie, Auf dem Hügel 69, 53121 Bonn, Germany
[2] University of California San Diego, Dept. of Physics, Center for Astrophysics and Space Sciences, Mail Code 0424, La Jolla, CA 92093-0424, USA
[3] National Astronomical Observatories, Chinese Academy of Science, Beijing 100012, PR China

Received 20 September 2002 / Accepted 15 January 2003

Abstract. We present the data from 11 observing campaigns (carried out between 1989 and 1999) at the Effelsberg 100 m radio telescope to study Intraday Variability in Active Galactic Nuclei. Most of these observations were performed in total power and linear polarization. We give summary tables, light curves, and structure functions from these data sets. Due to the large number of individual observations, only examples of the lightcurves will be presented here; the complete set of figures will be accessible online⋆⋆. Intraday variations are present in nearly all sources (detected during at least one of the observing campaigns). Variations in total flux density are usually accompanied by similar variability of the linear polarization. In most cases, the latter variations are stronger and faster by up to a factor of two.

Key words. galaxies: active – quasars: general – radio continuum: galaxies

1. Introduction

Since its discovery in 1985 (see, e.g. Witzel et al. 1986; Heeschen et al. 1987), Intraday Variability (IDV, i.e., flux-density variations on time-scales less than a day) has been shown to be a common, but complex, phenomenon among compact flat-spectrum extragalactic radio sources. Our earlier observations (Heeschen et al. 1987; Quirrenbach et al. 1992; and Quirrenbach et al. 2000, hereafter Paper I), show that IDV is detected in a large fraction of this class of sources. Amplitude variations of up to a factor of two have been reported in the radio regime as well as in the optical bands (e.g. Quirrenbach et al. 1992; Wagner & Witzel 1995). Dennett-Thorpe & de Bruyn (2000) reported even stronger variability (up to a factor of 2–3 within less than one hour) in J1819+3845. Observations of IDV have also been carried out in the southern hemisphere (Kedziora-Chudczer et al. 1997, 2001).

The occurrence and strength of IDV is related to the milliarcsecond-scale structure of the sources: it is very common in objects dominated by a compact VLBI core, but normally is not found or only weakly present in sources with a prominent VLBI jet (Quirrenbach et al. 1992). In parallel to the variability of the total flux density, variations of the polarized flux density and the polarization angle are observed frequently in many sources (Quirrenbach et al. 1989; Gabuzda et al. 2000a,b; Kraus et al. 1999a,b,c). Both correlations (e.g. in 0716+714) and anti-correlations (e.g. in 0917+624) between the total and the polarized flux density variations have been seen (Wegner 1994). However, this behavior can change between different observations of the same source. In two sources, 0716+714 and 0954+658, there is evidence for a correlation between the rapid flux density variability in the radio and the optical regime (Quirrenbach et al. 1991; Wagner et al. 1993). Such an effect would severely constrain any model for the interpretation of IDV and rule out propagation effects as the dominant cause of IDV.

From light travel time arguments, it is clear that IDV – if it is intrinsic to the source – originates from very small regions of the AGN (light days to light hours). In this case, it would impliy apparent brightness temperatures of up to 10^{19} K, far in excess of the inverse Compton limit of 10^{12} K (Kellermann & Pauliny-Toth 1969). Models to deal with this problem are briefly discussed in the last section.

In this paper, we present results from eleven observing campaigns carried out in order to study intraday variations in

Send offprint requests to: A. Kraus,
e-mail: akraus@mpifr-bonn.mpg.de
⋆ *Present address:* Landessternwarte Heidelberg, Königstuhl, 69117 Heidelberg, Germany.
⋆⋆ The figures of the Appendix are only available in electronic form at http://www.edpsciences.org

Table 1. Summary of experiments. In all experiments, except in December 1991 and September 1998 (at $\nu = 32$ GHz), we obtained information on both the total intensity and the linear polarization variability.

date	frequencies [GHz]	N
22/12/1989 – 29/12/1989	4.75, 10.55	6
31/07/1990 – 03/08/1990	2.70, 4.75	8
17/05/1991 – 24/05/1991	2.70, 4.75	11
27/12/1991 – 03/01/1992	2.70, 4.75, 10.55	10
10/04/1993 – 13/04/1993	4.75	3
18/06/1993 – 20/06/1993	4.75	4
01/09/1995 – 08/09/1995	2.70, 4.85	4
05/12/1997 – 08/12/1997	4.85, 10.45	4
25/12/1997 – 31/12/1997	2.70, 4.85, 10.45	9
17/09/1998 – 22/09/1998	4.85, 10.45, 32	5
08/02/1999 – 14/02/1999	4.85	5

Notes: The number N gives the number of target sources observed (i.e., the steep-spectrum calibrators are not included).

a sample of compact, flat-spectrum[1], radio sources. Between 1989 and 1999 we used the 100 m Effelsberg radio telescope of the MPIfR to observe 29 flat-spectrum radio sources at frequencies ranging from 2.7 to 32 GHz (see Table 1). The observed sources which all belong to the 1-Jy catalog (Kühr et al. 1981) were selected mainly on the basis of exhibiting an interesting behavior in earlier observations (e.g. Quirrenbach et al. 1992). Several sources were observed repeatedly, to study in more detail their variability characteristics (and its change with time). Together with our earlier measurements (Heeschen et al. 1987; Quirrenbach et al. 1992, Paper I), we have now investigated the complete sample of flat-spectrum radio sources of the 1-Jy catalog with declinations $\geq 60°$. This sample consists of 22 sources; here we present results for 16 of these sources.

In the next sections the observations and data reduction procedures are described, and the methods of statistical analysis are introduced. The properties of all program sources are listed in Table 2. All results are summarized in a tabular form, and for selected program sources the light curves are shown. Throughout the paper we make no assumption on the physical origin of IDV, but at the end we briefly comment on currently discussed models.

Some of the data sets observed in the program have been discussed in more detail in previous publications (e.g. Krichbaum et al. 1991; Kraus et al. 1999a,b,c). A statistical analysis of the entire database, and a more detailed interpretation will be given in a forthcoming paper (Cimò et al., in preparation). Discussions about specific sources, and the comparision of our results with observations at other wavelengths will also follow.

2. Observations and data reduction

All of the observed sources are point-like and quite bright ($\gtrsim 0.5$ Jy)[2] within the range of frequencies observed. This allows flux densities to be determined with "cross-scans" (Heeschen et al. 1987; Quirrenbach et al. 1992) through the source position. These cross-scans consisted of 8–20 (depending on the observing frequency and the source strength) individual subscans. Half of these subscans were performed in azimuth and elevation, respectively. This enables us to check the position offsets in both coordinates. Lefthand- and righthand-circular polarization signals are fed into a polarimeter, giving measurements of the total intensity (i.e., Stokes-parameter I) and the linear polarization (i.e., Stokes-parameters Q and U) of the sources simultaneously. During the observing campaigns, an individual source was observed every 0.5–4 hours (depending on the total number of sources and frequencies observed in each campaign).

2.1. Total intensity data

As the first step of the data analysis, a Gaussian profile is fitted to every subscan. The amplitude of these Gaussians (which are the result of the convolution of the point-like brightness distribution of the source with the antenna beam) is a measure of the flux density of the source. After applying a correction for small pointing offsets, the amplitudes of all individual subscans in one cross-scan are averaged. At $\lambda = 9$ mm and for the polarization analysis, the subscans of one direction (azimuth or elevation) were averaged before fitting the gaussian. Subsequently, we correct the measurements for the elevation-dependent sensitivity of the antenna and systematic time-dependent effects, using secondary calibrators close to the program sources (e.g. steep-spectrum sources like 0951+699). These objects are known to show no variations on short timescales (see, e.g. Heeschen et al. 1987). At $\lambda = 9$ mm, we additionally determine the opacity of the atmosphere and correct each measured flux density for the atmospheric attenuation.

Finally, we link our observations to the absolute flux density scale (Baars et al. 1977; Ott et al. 1994), by using frequently observed primary calibrators like 3C286, 3C48, and NGC7027. The final measurement errors are derived from the formal statistical errors and a contribution from the residual fluctuations of the non-variable secondary calibrators. The resulting measurement uncertainties usually lie in the range of 0.3–1% at $\lambda = 11,6$ cm; for the shorter wavelengths they were somewhat higher (1–4% depending e.g. on weather conditions).

2.2. Linear polarization data

For the analysis of the linear polarization data, Gaussian profiles are fitted to the signal observed in the Stokes-channels Q and U that describe the linear polarization of the observed source[3]. In order to correct for the various instrumental effects, we use the method presented by Turlo et al. (1985). Different amplifications of Q and U, instrumental polarization and cross-talk, etc., are parametrized by a 3×3-matrix $\underline{\mathbf{M}}$. A second

[1] As we adopt $S \propto \nu^{\alpha}$ throughout the paper, this corresponds to $\alpha \geq -0.5$.

[2] Several sources are at present weaker than the original 1-Jy limit.

[3] We neglect any circular polarization here (which is $\leq 0.5\%$ for all sources, Weiler & de Pater 1983; Homan et al. 2001). Hereafter, when we mention polarization, linear polarization is always meant.

matrix $\underline{\mathbf{P}}$ (a rotation matrix with the parallactic angle as parameter) takes into account the parallactic rotation of the polarization vector. To describe the observation process (i.e., to get the observed flux density and linear polarization), both matrices are multiplied by the (a priori unknown) flux density vector $\boldsymbol{S}$ with the true Stokes parameters of the source:

$$\boldsymbol{S}_{\rm obs} = \begin{pmatrix} I_{\rm obs} \\ Q_{\rm obs} \\ U_{\rm obs} \end{pmatrix} = \underline{\mathbf{M}} \cdot \underline{\mathbf{P}} \cdot \begin{pmatrix} I \\ Q \\ U \end{pmatrix} = \underline{\mathbf{M}} \cdot \underline{\mathbf{P}} \cdot \boldsymbol{S}. \quad (1)$$

To derive the true values of $\boldsymbol{S}$ from the observed $\boldsymbol{S}_{\rm obs}$, Eq. (1) has to be inverted. To do that, we determine the elements of $\mathbf{M}$ by least-square-fits to $\boldsymbol{S}_{\rm obs}$ using suitable calibrator sources for which we know the true flux density and polarization. Beside the main polarization calibrator 3C286, we have also used 0836+710. This source has a high degree of polarization (~9% at $\lambda = 6$ cm) and usually shows no short time-scale variability. In addition, an unpolarized (non-variable) source (e.g. 0951+699) has been included to improve the accuracy of the determination of the instrumental polarization (which is of the order of 0.5% for $\lambda = 6$ cm).

The first step of the polarization analysis may have introduced a spurious polarization signal into the Stokes parameters Q and U (noise bias caused by fitting a Gaussian to an unpolarized source). We estimate this noise bias to be ≤2 mJy, and therefore we consider all sources with a mean polarized flux density ≤6 mJy as unpolarized and exclude those sources from the investigation of polarization variability.

The final measurement errors for the linear polarization are usually in the range of 3–5% for the polarized flux density, and within 2–5° for the polarization angle.

During some of the observing runs we were not able to measure the polarization successfully because of either technical problems or bad weather conditions that severely increased the scatter in the data.

3. Statistical analysis

For the statistical analysis of the data, we use several quantities which are described in detail in Paper I. Here, we briefly summarize them:

The *modulation index m*

$$m[\%] = 100 \cdot \frac{\sigma_I}{< I >} \quad (2)$$

(with σ_I denoting the standard deviation of the flux density, $< I >$ its average in time) provides a measure of the strength of the observed amplitude variations without taking into account the error of the individual measurement. As a criterion whether a source is variable or not, we perform a Chi-Square-test (e.g. Bevington & Robinson 1992) with the reduced Chi-Square

$$\chi^2_r = \frac{1}{N-1} \sum_{i=1}^{N} \left(\frac{I_i - < I >}{\Delta I_i} \right)^2, \quad (3)$$

where N is the number of measurements, the I_i are the individual flux densities and ΔI_i their errors. This tests the hypothesis that the light curve could be modeled by a constant function. Only sources for which this probability is ≤0.1%, are considered to be variable.

Following Heeschen et al. (1987) and Quirrenbach et al. (1992), we define the *variability amplitude* for the variable sources as

$$Y[\%] = 3 \sqrt{m^2 - m_0^2}, \quad (4)$$

where m_0 is the modulation index of the non-variable sources observed in the same experiment. For non-variable sources, Y is set to zero.

For the polarized intensity P, the corresponding quantities are

$$m_P[\%] = 100 \cdot \frac{\sigma_P}{< P >}, \quad (5)$$

$$Y_P[\%] = 3 \sqrt{m_P^2 - m_{P,0}^2}; \quad (6)$$

and for the polarization angle χ, we use

$$m_\chi[^\circ] = \sigma_\chi, \quad (7)$$

$$Y_\chi[^\circ] = 3 \sqrt{\sigma_\chi^2 - \sigma_{\chi,0}^2}. \quad (8)$$

For P and χ, the Chi-Square-test is performed analogous to the total intensity. All statistical quantities are derived independently for each observing campaign.

Structure functions can be used to search for characteristic time-scales and periodicities. The first order structure function $D(\tau)$ is defined as (see Simonetti et al. 1985):

$$D(\tau) = < (I(t) - I(t+\tau))^2 >_t \quad (9)$$

with $< . >_t$ denoting averaging in time. Since our data are unevenly sampled, we derived the structure functions using an interpolation algorithm. For a given $I(t)$ a value for $I(t+\tau)$ was interpolated from two adjacent data points. The minimal interpolation intervall τ was choosen comparable to the sampling of the data. To assess the errors caused by the interpolation process, each structure function was derived twice, first by starting from the beginning of the time series, and second by starting at the end and proceeding backwards. These errors depend on the sampling of the light curve and the number of data points over which the averaging is done. Usually they lie in the range of a few percent.

A typical time-scale in the light curve (i.e., the time between a minimum and a maximum or vice versa) is indicated by a maximum in the structure function, while the presence of a period in the light curve causes a minimum in the structure function (e.g. Heidt & Wagner 1996). Following Heeschen et al. (1987), we use structure functions to define variability types, depending on the observed time-scale. A source whose structure function reaches a maximum within two days is called type II (i.e., a fast-varying source). Slower varying sources are assigned type I, non-variable sources type 0.

Table 2. Overview of the variability characteristics for the individual sources.

Source	opt.Id.	z	N	$\lambda_{\rm obs}$	max. Y_I	min. Y_I	$\lambda_{\rm maxY}$	Var. types	max. Y_P	min. Y_P
(1)	(2)	(3)	(4)	(5)	(6)	(7)	(8)	(9)	(10)	(11)
0454+844	BLL	0.112	2	11, 6, 2.8	9.9	0	11	0, I, II	–	–
0602+673	QSO	1.970	2	11, 6, 2.8, 0.9	4.0	0	6	0, I, II	72.5	0
0716+714	BLL	?	8	11, 6, 2.8. 0.9	16.4	0	6	0, I, II	76.6	0
0723+679	QSO	0.846	1	11, 6	0	0	–	0	0	0
0804+499	QSO	1.433	3	11, 6, 2.8	10.1	2.4	11	I, II	69.9	0
0828+493	BLL	0.548	1	11, 6, 2.8	14.7	5.1	11	II	–	–
0831+557	GAL	0.241	2	6	0	0	–	0	–	–
0833+585	QSO	2.101	1	11, 6	2.4	0	6	I	29.5	0
0836+710	QSO	2.172	11	11, 6, 2.8, 0.9	2.0	0	11	I, II	0	0
0850+581	QSO	1.322	1	6	1.9	0	6	I	0	0
0917+624	QSO	1.446	8	11, 6, 2.8, 0.9	16.2	0	6	0, I, II	113.5	20.7
0945+664	GAL	?	2	11, 6, 2.8	0	0	–	0	58.6	0
0954+556	QSO	0.901	1	11, 6	2.1	0	6	II	18.1	0
0954+658	BLL	0.367	5	11, 6, 2.8	7.8	3.5	11	I, II	71.9	0
1039+811	QSO	1.254	2	11, 6, 2.8	2.8	0	6	0, I, II	27.3	0
1150+812	QSO	1.250	1	11, 6, 2.8	1.6	0	11	0, I	19.1	0
1418+546	BLL	0.152	1	6, 2.8	3.5	3.3	2.8	II	14.3	0
1435+638	QSO	2.068	1	6, 2.8	1.5	0	6	I	10.4	0
1504+377	GAL	0.674	1	6	2.1	2.1	6	II	–	–
1637+574	QSO	0.750	1	11, 6	2.4	2.0	11	II	30.7	0
1739+522	QSO	1.379	1	11, 6	13.8	9.9	11	I, II	88.8	40.3
1749+701	BLL	0.770	1	11, 6	6.1	4.0	6	I, II	35.0	0
1803+784	BLL	0.684	3	11, 6, 2.8	6.1	2.1	11	I, II	23.5	9.5
1807+698	BLL	0.051	1	11, 6	1.6	0	11	II	18.3	0
1823+568	BLL	0.664	1	11, 6	6.7	6.0	6	I	51.2	21.5
1928+738	QSO	0.302	1	11, 6	0	0	–	0	20.7	0
1954+513	QSO	1.230	1	6	2.7	2.7	6	II	–	–
2007+777	BLL	0.342	2	11, 6, 2.8	5.3	0	6	0, I, II	35.5	0
2200+420	BLL	0.069	1	11, 6	3.9	2.3	11	I, II	18.6	18.0

Notes: Columns are: (1) - source name; (2) - optical identification (BLL: BL Lac objects, QSO: quasars, GAL: radio galaxies); (3) - redshift; (4) - Number of observing epochs; (5) wavelengths of the observations; (6), (7) - maximum and minimum observed variability amplitudes in total flux density of all epochs; (8) wavelength at which the maximum variability amplitude Y was observed; (9) observed variability types (total intensity); (10), (11) - maximum and minimum observed variability amplitudes for polarized intensity of all epochs (0: source was not variable, -: source was not observed or was unpolarized).

4. Results

An overview of our results (in terms of the variability amplitudes for total and polarized flux density, describing the strength of the IDV) is given in Table 2. Detailed results for each experiment are presented in Tables 3–13. These tables contain information for both total intensity and linear polarization. In the header we list for each wavelength the modulation indices for total and polarized intensity and the polarization angle; T is the duration of the campaign. For each source and each wavelength, the number of data points, the mean value of the intensity, the modulation index m, and the reduced χ^2_r is given (in total intensity as well as in polarized intensity and polarization angle). For variable sources the variability amplitude Y (Y_P, Y_χ, respectively) is presented. For total intensity also the variability type is given (from the structure function analysis described above).

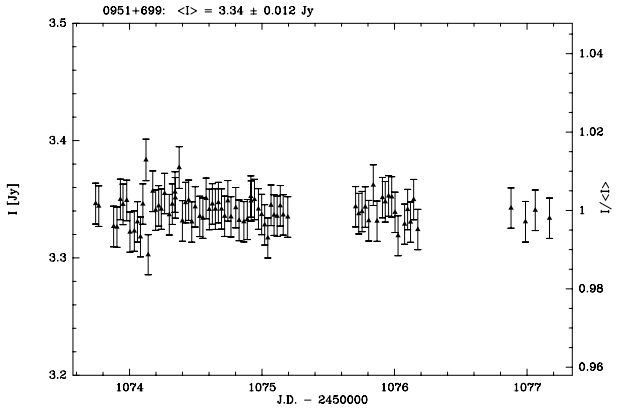

Fig. 1. Light curve of the secondary calibrator 0951+699 observed in September 1998 at $\lambda = 6$ cm. Note that, except for a few outliers (probably due to unfavorable weather conditions) at the beginning of the observation, all points lie within a ±0.5% range around the mean flux density ($m = 0.37\%$).

Because of the large number of sources observed, only a few light curves (Figs. 1–7) are presented in the printed version of the paper. The complete set of figures (light curves and structure functions of the variable sources) is accessible online at `http://www.edpsciences.org`.

Table 3. Observations from December 1989.

$\lambda = 6$ cm			$m_0 = 0.5\%$			$m_{P,0} = 1.5\%$			$\sigma_{\chi,0} = 0.5°$			$T = 6$ d		
$\lambda = 2.8$ cm			$m_0 = 1.2\%$			$m_{P,0} = 2.5\%$			$\sigma_{\chi,0} = 0.7°$					
Source	N	I [Jy]	m [%]	χ^2_r	Y [%]	type	P [Jy]	m_P [%]	χ^2_r	Y_P [%]	χ [°]	m_χ [°]	χ^2_r	Y_χ [°]
0716+714	33	0.56	5.5	112.7	16.4	I	0.020	16.4	18.8	48.9	8.2	2.8	4.5	8.1
	31	0.62	3.1	5.5	8.6	I	0.018	13.5	7.5	39.8	−0.5	4.2	9.4	12.3
0836+710	61	2.13	0.5	0.7		0	0.196	1.6	0.6		102.9	0.4	0.4	
	58	1.83	1.4	1.1		0	0.120	2.7	0.7		107.9	0.8	1.3	
0917+624	111	1.50	5.4	104.0	16.2	II	0.021	33.7	83.6	101.0	22.8	9.9	43.6	29.7
	109	1.69	4.1	9.9	11.9	II	0.017	26.9	24.2	80.5	53.1	14.2	102.3	42.6
0954+658	32	1.32	1.3	6.6	3.7	II	0.127	2.8	1.4		−23.1	0.8	1.2	
	29	1.31	2.2	2.8	5.4	II	0.130	3.3	1.1		−22.6	0.7	1.2	
1803+784	22	3.06	0.9	3.3	2.3	II	0.112	3.5	2.6	9.5	87.1	0.9	1.5	
	19	3.36	2.3	3.3	6.0	II	0.106	7.1	4.7	20.0	102.4	1.5	5.1	4.1
2007+777	20	1.71	1.8	11.9	5.3	I	0.057	5.0	4.2	14.2	92.2	1.1	1.8	
	20	2.30	2.0	2.4	4.8	II	0.143	3.3	1.2		94.8	0.9	2.0	

Table 4. Observations from July 1990.

$\lambda = 11$ cm			$m_0 = 0.2\%$			$m_{P,0} = 1.3\%$			$\sigma_{\chi,0} = 0.8°$			$T = 3$ d		
$\lambda = 6$ cm			$m_0 = 0.5\%$			$m_{P,0} = 1.3\%$			$\sigma_{\chi,0} = 1.0°$					
Source	N	I [Jy]	m [%]	χ^2_r	Y [%]	type	P [Jy]	m_P [%]	χ^2_r	Y_P [%]	χ [°]	m_χ [°]	χ^2_r	Y_χ [°]
0804+499	13	0.93	1.7	18.0	4.9	II	0.016	23.3	3.6	69.9	107.2	11.4	9.6	34.2
	12	0.93	1.4	7.1	3.8	II	0.015	8.9	2.6		102.1	5.2	8.0	15.4
0836+710	16	2.85	0.3	1.5		0	0.231	2.5	1.2		99.0	0.8	1.1	
	18	2.16	0.7	2.0		0	0.199	1.9	1.1		103.1	0.7	0.6	
1749+701	17	0.63	1.4	8.2	4.0	II	0.021	11.7	1.2		125.2	3.7	2.1	
	17	0.59	2.1	15.3	6.1	I	0.015	11.8	4.7	35.0	111.8	3.7	4.4	10.7
1803+784	16	2.22	1.0	13.2	2.8	I	0.078	5.4	2.5	15.7	54.0	2.7	5.6	7.6
	19	2.35	0.9	2.9	2.1	I	0.065	4.0	3.2	11.5	91.0	1.6	2.8	3.9
1807+698	13	2.00	0.6	4.7	1.6	II	0.052	6.2	2.2		−3.9	3.0	3.9	8.6
	17	1.87	0.4	0.6		0	0.035	6.2	4.4	18.3	31.3	2.9	6.0	8.3
1928+738	15	3.62	0.2	0.8		0	0.109	4.2	2.3		112.0	1.3	1.9	
	16	3.69	0.5	0.9		0	0.075	7.0	8.9	20.7	82.9	2.3	5.7	6.2
2007+777	14	1.23	0.5	2.9	1.4	II	0.058	11.9	8.3	35.5	82.5	2.5	4.3	7.2
	15	1.39	0.8	2.4		0	0.083	3.9	3.7	11.2	89.5	1.9	4.2	5.0
2200+420	11	2.70	1.3	25.6	3.9	I	0.085	6.3	4.1	18.6	88.9	2.9	6.5	8.4
	10	3.05	0.9	3.4	2.3	II	0.093	6.1	7.6	18.0	4.3	1.8	3.6	4.4

As an example of a non-variable source (which was used for correcting for instrumental effects and elevation and time dependencies of the antenna sensitivity) we show the light curve of 0951+699 in Fig. 1. Its modulation index was 0.37%.

In September 1998, we investigated 5 sources at 32 GHz in order to search for short time-scale variations at a high frequency (Table 12, Fig. 3). Although the scatter in the data is quite high ($m_0 = 3.0\%$), clear evidence for IDV in 0716+714 was found. In the case of 0602+673 and 0917+624, there is a some evidence that variability is present (probably heavily undersampled), but the adopted statistical criterion qualifies these sources as non-variable. Future observations with better time-sampling are needed to confirm this.

5. Individual sources

In this section we briefly summarize specific properties of some of the more remarkable flat-spectrum sources observed (see also Paper I). The optical identifications and redshifts are taken from Kühr et al. (1981) and Stickel et al. (1994).

1. 0454+844: A BL Lac object which since the observation of the 1-Jy catalog (Kühr et al. 1981) displayed a strong flux density decrease (in 1997: $I \simeq 0.3$ Jy at $\lambda = 6$ cm). This source was observed twice in December 1997, and IDV was detected.
2. 0602+673: This quasar was observed in December 1997 and September 1998 and mostly showed pronounced type-II variations (Fig. 2). In 0602+673, as in several other sources, the variability in polarized intensity is faster than in total intensity: the variability time-scale is about 2 days in total flux density, and about half a day in polarization.
3. 0716+714: This BL Lac object (with unknown redshift) is one of the most frequently observed sources. In nearly all observations it has shown pronounced variations at all frequencies in both total intensity and in linear polarization (e.g. Wagner et al. 1993). There is a direct correlation between the flux density at various frequencies, and between total and polarized flux density. In this source, IDV at 32 GHz was detected in September 1998 (Fig. 3).

Table 5. Observations from May 1991.

$\lambda = 11$ cm			$m_0 = 0.4\%$			$m_{P,0} = 2.3\%$		$\sigma_{\chi,0} = 2.0°$			$T = 7$ d			
$\lambda = 6$ cm			$m_0 = 0.5\%$			$m_{P,0} = 1.5\%$		$\sigma_{\chi,0} = 1.5°$						
Source	N	I [Jy]	m [%]	χ^2_r	Y [%]	type	P [Jy]	m_P [%]	χ^2_r	Y_P [%]	χ [°]	m_χ [°]	χ^2_r	Y_χ [°]
0716+714	39	0.60	3.2	13.7	9.6	II	0.013	25.4	1.6		−2.1	6.9	1.4	
	47	0.54	5.1	81.6	15.2	II	0							
0833+585	37	0.69	1.1	1.8		0	0.015	20.5	1.4		−13.5	6.1	1.5	
	37	0.62	1.0	3.0	2.4	I	0.020	10.0	3.9	29.5	−6.9	2.8	1.9	
0836+710	40	2.86	0.4	0.7		0	0.222	5.2	1.0		99.0	2.8	1.2	
	39	2.14	0.4	0.6		0	0.196	1.7	0.8		102.7	1.4	0.9	
0850+581	33	1.04	1.3	4.2	3.7	I	0.025	15.1	1.9		68.1	6.4	3.1	18.1
	37	1.01	0.5	0.7		0	0							
0954+556	37	2.57	0.6	1.6		0	0.052	9.8	1.8		8.9	3.8	1.8	
	34	2.08	0.9	2.6	2.1	II	0.059	6.2	5.9	18.1	6.1	2.1	1.7	
0954+658	36	1.10	2.2	14.3	6.5	I	0.081	6.6	1.3		−29.7	2.5	0.9	
	37	1.12	1.6	8.5	4.4	I	0.115	3.2	2.5	8.5	−18.3	1.3	0.7	
1418+546	34	1.33	1.2	4.6	3.3	II	0.046	9.2	1.7		67.3	3.7	1.6	
	36	1.42	1.3	5.7	3.5	II	0.040	5.0	2.4	14.3	60.0	3.0	3.3	7.9
1637+574	35	1.30	0.9	2.7	2.4	II	0.029	13.1	1.7		95.9	4.4	1.7	
	34	1.38	0.8	2.4	2.0	II	0.027	10.3	6.2	30.7	115.3	3.7	3.3	10.0
1739+522	35	2.20	4.6	111.9	13.8	II	0.025	29.7	6.6	88.8	7.6	7.5	4.1	21.8
	35	2.57	3.3	46.8	9.9	I	0.059	13.5	33.2	40.3	19.9	4.1	6.5	11.4
1803+784	36	2.31	2.1	20.6	6.1	I	0.099	8.2	2.5	23.5	50.2	2.7	1.1	
	36	2.42	1.7	9.9	4.8	II	0.095	5.6	6.2	16.2	85.1	1.7	1.3	
1823+568	35	1.31	2.1	14.5	6.0	I	0.025	17.2	3.0	51.2	42.1	5.1	1.8	
	36	1.28	2.3	18.0	6.7	I	0.051	7.3	5.6	21.5	45.4	3.2	3.9	8.5

The fastest IDV seen in our campaigns was observed in this source in April 1993 at $\lambda = 6$ cm (Fig. 4): variations on a time-scale of about two hours occured in addition to variability on longer time scales. This indicates the presence of more than one distinct time scale in the data which could be confirmed by a power-spectrum analysis.

4. 0804+499: In data obtained in April 1990, this quasar showed the highest variability amplitude (∼35% at $\lambda = 6$ cm) observed so far in our sample (Quirrenbach et al. 1992). Afterwards, rapid variability was observed several times (see also Paper I), although on a level of "only" a few percent.
5. 0836+710: Weak and slow variations have been seen in this quasar only in September 1995 and September 1998. In all other experiments (including all the earlier ones), this object did not exhibit any measurable variation. This behavior is not surprising because this source has a prominent VLBI jet (e.g. Otterbein et al. 1998; Lobanov et al. 1998) which contributes significantly to the total flux density. In most experiments it was used as one of the secondary calibrators; it is particularly useful as a polarization calibrator (see Sect. 2).
6. 0917+624: One of the most strongly variable sources in total flux density and linear polarization (P and χ; e.g. Quirrenbach et al. 1989; Kraus et al. 1999b). It was observed several times, and usually showed pronounced IDV (of type II) which seems to be directly correlated at wavelengths $2 \leq \lambda \leq 11$ cm. The polarized flux density of 0917+624 is usually anti-correlated with the total flux density (see Figs. 5 and 6)[4]. In September 1998, a remarkable change of the variability properties was observed. Instead of the strong variations on time-scales of about one day, 0917+624 displayed only a monotonic increase over the five day observing period. In February 1999 the source returned to its original fast variability state (Kraus et al. 1999c). Afterwards, the variability ceased again (Fuhrmann et al. 2002). Both intrinsic variations (Qian et al. 1991) and propagation effects in the interstellar medium (Rickett et al. 1995; Rickett et al. 2001) have been explored as potential causes of IDV in this source.
7. 0954+658: A BL Lac object ($z = 0.367$) showing weak variability on a level of a few percent. This is one of the few sources in which variability occured whenever it was investigated. In March 2000, Cimò et al. (2002) observed a very rapid flux density dip (∼10% within one day) resembling an extreme scattering event (e.g. Fiedler et al. 1994), but on a much shorter time scale. A similar behavior was observed in the BL Lac object 1749+701 (Heeschen et al. 1987) and in the quasar 1739+522 (see below and Fig. 7).

[4] Cross correlation techniques are described in more detail by Edelson & Krolik (1988) and White & Peterson (1994). The correlations in 0917+624 are also discussed by Quirrenbach et al. (1989).

Table 6. Observations from December 1991; only total intensity.

$\lambda = 11$ cm		$m_0 = 0.4\%$			$T = 7$ d	
$\lambda = 6$ cm		$m_0 = 0.6\%$				
$\lambda = 2.8$ cm		$m_0 = 0.7\%$				
Source	N	I [Jy]	m [%]	χ^2_r	Y [%]	type
0716+714	48	0.62	3.1	19.1	9.3	I
	56	0.55	3.2	24.1	9.4	I
	48	0.53	2.0	6.5	5.5	II
0804+499	46	0.90	3.4	33.4	10.1	II
	57	0.87	2.4	16.0	7.0	II
	49	0.82	2.5	9.7	7.2	II
0828+493	18	0.32	4.9	14.9	14.7	II
	41	0.32	2.4	10.5	7.0	II
	38	0.32	1.8	3.7	5.1	II
0831+557	–					
	37	5.53	0.6	1.1		0
	–					
0836+710	46	2.77	0.5	1.1		0
	47	2.11	0.7	1.4		0
	41	1.71	0.5	0.4		0
0917+624	61	1.10	2.6	22.9	7.8	II
	62	1.19	2.7	20.4	7.7	II
	59	1.59	1.8	5.2	5.1	II
0945+664	–					
	42	1.21	0.6	1.0		0
	–					
0954+658	41	0.92	2.3	14.8	6.7	I
	43	0.86	1.6	7.4	4.5	I
	40	0.86	1.7	4.4	4.5	I
1504+377	–					
	29	0.86	0.9	2.4	2.1	II
	–					
1954+513	–					
	40	1.68	1.1	3.6	2.7	II
	–					

8. 1739+522: This quasar was observed in May 1991. In addition to variations on a few percent level, a rapid flux density dip has been seen at $\lambda = 11,6$ cm (see, e.g. Fig. 7, upper panel) which – as in 0954+658 (see before) – could be interpreted as an extreme scattering event.
9. 1803+784: This source (classified variously as BL Lac object or quasar, $z = 0.684$) is dominated by a long VLBI jet (Britzen et al. 2001 and references therein) and exhibits only slow variability (type I) in most observations.
10. 2007+777: A BL Lac object showing mostly slow variations. Peng et al. (2000) studied the broad band variability characteristics in this object (at radio, infrared, and optical wavelengths) and found variations on time-scales of days to weeks with variability amplitudes increasing monotonically with frequency.

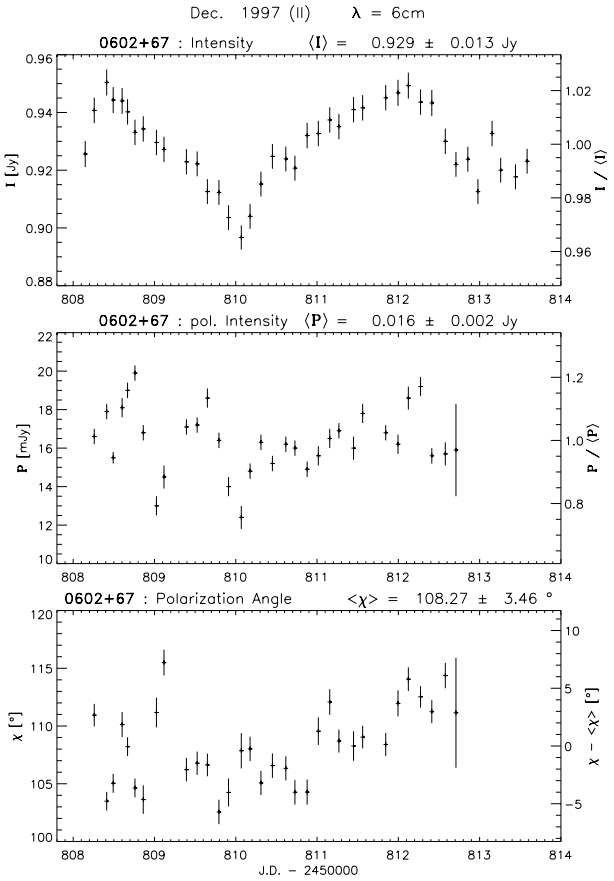

Fig. 2. Light curve of 0602+673 in December 1997. IDV with a timescale of about 2 days is clearly seen in total intensity, whereas in polarized intensity the variability is much faster. Close to the end of the observing run, we were not able to get reliable polarization data due to technical problems.

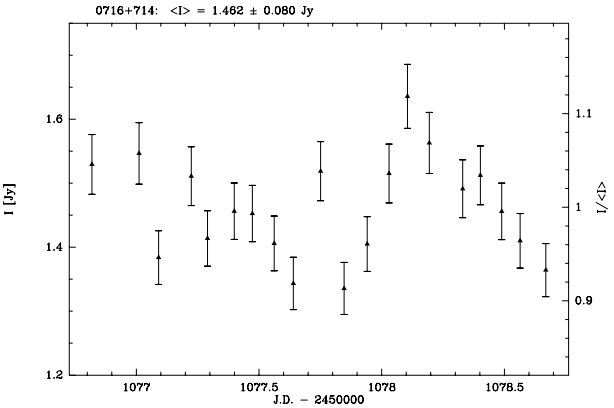

Fig. 3. Light curve of BL 0716+714 in September 1998 at $\lambda = 9$ mm. Despite the high scatter in the data, IDV with a peak-to-peak amplitude of about 20% is clearly visible.

6. Discussion

We have presented data from 11 observing campaigns carried out with the Effelsberg 100 m radio telescope to investigate the intraday variability of compact extragalactic flat-spectrum radio sources. In total we have observed 29 flat-spectrum sources (several repeatedly). Our observations reveal that nearly all of these sources show IDV (detected during at least one of the observing campaigns) and only four sources never exhibit any variability in total intensity (see Table 2). One should note, that those sources were observed less often than others, and that sources reveal changes in their variability properties between different epochs. Hence, it is quite possible that those sources could display variations when observed again.

Table 7. Observations from April 1993.

$\lambda = 6$ cm			$m_0 = 0.4\%$			$m_{P,0} = 1.5\%$			$\sigma_{\chi,0} = 0.5°$			$T = 3$ d			
Source	N	I [Jy]	m [%]	χ^2_r	Y [%]	type	P [Jy]	m_P [%]	χ^2_r	Y_P [%]	χ [°]	m_χ [°]	χ^2_r	Y_χ [°]
0716+714	193	0.63	2.4	23.1	7.2	II	0.025	10.9	6.0	32.3	13.9	2.7	6.7	8.1
0836+710	202	2.26	0.4	0.9		0	0.206	1.9	1.0		101.1	0.4	0.9	
0917+624	196	1.52	1.4	9.9	4.2	I	0.015	14.9	3.5	44.5	72.6	3.7	3.7	11.1

Table 8. Observations from June 1993.

$\lambda = 6$ cm			$m_0 = 0.5\%$			$m_{P,0} = 1.3\%$			$\sigma_{\chi,0} = 0.3°$			$T = 2$ d			
Source	N	I [Jy]	m [%]	χ^2_r	Y [%]	type	P [Jy]	m_P [%]	χ^2_r	Y_P [%]	χ [°]	m_χ [°]	χ^2_r	Y_χ [°]
0804+499	115	1.29	1.0	3.5	2.4	I	0.040	4.6	1.5	13.2	92.9	1.5	3.0	4.5
0836+710	181	2.26	0.4	0.7		0	0.204	1.3	1.2		101.2	0.3	1.0	
0850+581	180	0.99	0.8	2.5	1.9	I	0							
0917+624	186	1.59	3.3	42.8	9.7	II	0.010	36.3	7.1	108.9	71.9	18.0	22.3	54.1

Table 9. Observations from September 1995.

$\lambda = 11$ cm			$m_0 = 0.4\%$			$m_{P,0} = 2.0\%$			$\sigma_{\chi,0} = 0.8°$			$T = 7$ d			
$\lambda = 6$ cm			$m_0 = 0.9\%$			$m_{P,0} = 4.0\%$			$\sigma_{\chi,0} = 2.0°$						
Source	N	I [Jy]	m [%]	χ^2_r	Y [%]	type	P [Jy]	m_P [%]	χ^2_r	Y_P [%]	χ [°]	m_χ [°]	χ^2_r	Y_χ [°]
0716+714	72	0.53	3.7	32.3	11.1	I	0.014	20.3	1.1		0.4	7.5	1.7	22.3
	72	0.45	4.5	13.6	13.3	I	0.010	24.9	8.8	73.8	17.3	6.7	6.1	19.2
0723+679	70	1.31	0.3	0.5		0	0.043	6.2	1.0		−22.0	2.4	1.3	
	70	0.87	1.1	0.9		0	0.034	7.7	1.4		−9.4	2.5	1.5	
0836+710	72	2.81	0.8	3.4	2.0	II	0.223	2.1	1.1		99.8	0.7	0.4	
	70	2.06	0.9	0.7		0	0.176	5.6	0.8		104.9	1.0	0.3	
0954+658	70	0.54	2.6	16.3	7.8	II	0.030	10.7	1.3		−7.5	3.9	2.0	11.4
	70	0.55	2.4	4.4	6.7	I	0.032	8.9	2.0	23.7	−10.7	2.7	1.8	5.5

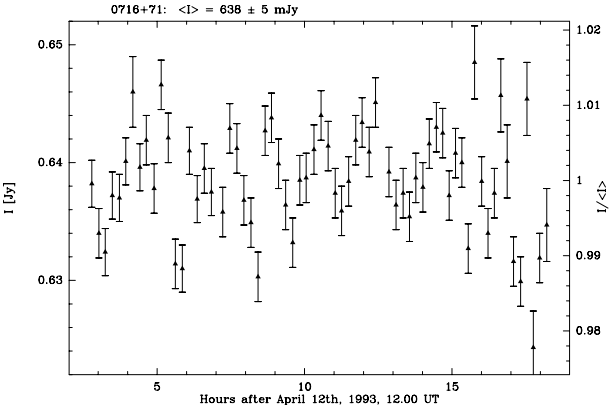

Fig. 4. Variability on very short time-scales in 0716+714 in April 1993 at $\lambda = 6$ cm. For better visibility, the data was smoothed slightly. Though weak, variations on time-scales of less than two hours are clearly visible. This light curve is part of a larger data set.

Very fast variations (i.e., on time-scales ≤2 days, type II) occur in about 40% of all observed light curves. This confirms that IDV occurs in a significant number of compact flat-spectrum radio sources, although the detailed variability characteristics may vary strongly from one object to another. As shown by Krichbaum et al. (2002), the dependence of the variability amplitude with frequency shows a different behavior for different sources, and could also vary between individual observations. The example of 0716+714 shows that there might be more than one distinct time-scale present in the light curves.

Variations in total flux density are usually accompanied by variability of the linear polarization. In most cases, the latter variations are stronger and faster by up to a factor of two. Few sources show variability in linear polarization although they are non-variable in total flux density.

The observations presented in this paper provide the last piece for forming a statistically complete sample of compact radio sources studied for IDV. The total sample, comprising the present observations and data from Paper I, Quirrenbach et al. (1992), and Heeschen et al. (1987), covers all flat-spectrum sources in the 1-Jy catalog (Kühr et al. 1981) with declinations $\delta \geq 60°$ (22 sources). A more detailed statistical analysis of the combined data sets will be presented in a future paper.

Since the discovery of IDV a large number of models have been developed to explain this phenomenon. Assuming an intrinsic origin of the variability, the size of a variable source can be derived from the variability time-scale using the light travel time argument. In this case, the linear size cannot be much larger than $c\,\Delta t$. Intraday variations with time-scales shorter than 2 days (as presented here) imply minimum brightness temperatures of 10^{16}–10^{19} K (e.g. Wagner & Witzel 1995). Therefore, IDV would cause a severe violation of the inverse Compton limit of 10^{12} K (Kellermann & Pauliny-Toth 1969). We note that for the standard shock-in-jet model, the observed (variability) brightness temperatures should be reduced by a

Table 10. First observations from December 1997.

$\lambda = 6$ cm			$m_0 = 0.4\%$			$m_{P,0} = 1.5\%$			$\sigma_{\chi,0} = 0.5°$			$T = 3$ d		
$\lambda = 2.8$ cm			$m_0 = 0.8\%$			$m_{P,0} = 4.0\%$			$\sigma_{\chi,0} = 1.5°$					
Source	N	I [Jy]	m [%]	χ^2_r	Y [%]	type	P [Jy]	m_P [%]	χ^2_r	Y_P [%]	χ [°]	m_χ [°]	χ^2_r	Y_χ [°]
0454+844	40	0.28	1.1	4.9	3.1	II	0							
	42	0.25	1.3	2.3	2.9	I	0							
0836+710	48	2.17	0.4	0.9		0	0.175	1.6	0.6		102.9	0.5	1.5	
	44	2.53	0.7	0.9		0	0.112	4.0	0.9		106.1	1.1	0.6	
0917+624	44	1.42	3.9	99.4	11.7	II	0.033	27.3	102.8	81.7	39.2	5.4	49.2	16.0
	42	1.36	1.6	4.7	4.1	II	0.016	26.6	21.1	78.8	41.4	8.0	10.3	23.5
1039+811	45	0.82	0.7	3.6	1.8	II	0							
	42	1.14	0.7	1.0		0	0.021	9.9	4.0	27.3	47.8	3.0	2.9	7.9

Table 11. Second observations from December 1997.

$\lambda = 11$ cm			$m_0 = 0.5\%$			$m_{P,0} = 2.5\%$			$\sigma_{\chi,0} = 1.0°$			$T = 6$ d		
$\lambda = 6$ cm			$m_0 = 0.5\%$			$m_{P,0} = 1.0\%$			$\sigma_{\chi,0} = 0.7°$					
$\lambda = 2.8$ cm			$m_0 = 0.8\%$			$m_{P,0} = 4.0\%$			$\sigma_{\chi,0} = 2.0°$					
Source	N	I [Jy]	m [%]	χ^2_r	Y [%]	type	P [Jy]	m_P [%]	χ^2_r	Y_P [%]	χ [°]	m_χ [°]	χ^2_r	Y_χ [°]
0454+844	19	0.29	3.4	26.8	9.9	I	0							
	23	0.28	2.4	19.3	7.2	II	0							
	11	0.24	0.7	0.6		0	0							
0602+673	41	0.75	1.2	5.3	3.1	II	0.014	13.0	1.3		96.5	4.3	1.8	
	40	0.93	1.4	9.4	4.0	II	0.016	10.3	12.8	30.8	108.3	3.5	11.0	10.2
	33	0.98	1.4	3.0	3.5	I	0.018	11.4	5.8	32.0	133.0	3.4	5.5	8.3
0716+714	28	0.66	2.9	34.2	8.7	I	0.017	25.7	7.8	76.6	19.2	6.4	2.8	19.0
	31	0.61	2.3	22.6	6.7	I	0							
	27	0.57	1.0	1.3		0	0							
0836+710	42	2.69	0.6	1.4		0	0.216	1.5	0.4		99.9	0.3	0.1	
	42	2.23	0.6	1.3		0	0.177	1.5	0.5		102.5	0.4	0.3	
	37	2.51	0.8	1.0		0	0.109	2.6	0.7		106.1	0.7	0.4	
0917+624	42	1.35	5.2	116.8	15.5	II	0.033	27.7	31.1	82.8	36.7	6.0	6.8	17.6
	43	1.45	5.2	123.6	15.4	II	0.031	32.4	163.5	97.2	37.2	6.8	20.6	20.3
	35	1.38	2.7	10.7	7.6	II	0.014	24.8	17.8	73.3	41.5	4.6	6.6	12.4
0945+664	40	1.69	0.5	1.1		0	0.028	9.4	2.0	27.3	131.0	1.9	0.5	
	42	1.21	0.5	1.1		0	0.031	3.6	1.8		132.6	0.8	0.9	
	34	0.69	0.9	1.3		0	0.011	12.7	3.7	36.1	79.2	3.1	2.5	7.2
1039+811	21	0.74	1.0	4.1	2.6	I	0							
	22	0.85	1.1	5.1	2.8	I	0							
	17	1.14	1.0	1.5		0	0.021	7.3	2.7	18.4	49.2	2.4	3.2	4.2
1150+812	18	1.55	0.7	2.4	1.6	I	0.027	8.2	1.7		117.3	2.6	1.4	
	21	1.52	0.7	2.3	1.5	I	0.024	6.4	5.2	19.1	88.1	2.0	3.6	5.6
	16	1.43	0.7	0.7		0	0.035	5.0	1.8		87.0	1.1	0.9	
1435+638	–													
	43	1.09	0.7	2.3	1.5	I	0.033	3.6	2.4	10.4	−23.6	0.9	0.9	
	35	0.96	0.8	1.3		0	0.028	4.9	1.7		−23.7	1.5	1.6	

factor $\sim\mathcal{D}^3$ (Blandford & Königl 1979; Blandford 1990) to obtain the brightness temperature in the source frame. Hence, to lower the brightness temperature to the inverse Compton limit, Doppler factors of order 20–200 would be required. This poses severe theoretical problems (e.g. Begelman et al. 1994). Studies of the VLBI kinematics in large source samples show that such high Doppler factors are unlikely (e.g. Witzel et al. 1988; Ghisellini et al. 1993), although in a few sources there is evidence for Lorentz factors of up to 20–30 (e.g. Jorstad et al. 2001; Romero et al. 2000). In cases of a special (non-spherical) geometry (e.g. Qian et al. 1991, 1996), the factor for the reduction of the brightness temperature could be of the order $\sim\mathcal{D}^5$; consequently lower Doppler factors are needed to meet the inverse Compton limit. Spada et al. (1999) discuss a model in which the radiating electrons are accelerated by shocks in a conical, oblique geometry. If the injection times are shorter

Table 12. Observations from September 1998; for $\lambda = 0.9$ cm only total power.

$\lambda = 6$ cm		$m_0 = 0.6\%$			$m_{P,0} = 1.5\%$		$\sigma_{\chi,0} = 0.8°$				$T = 5$ d			
$\lambda = 2.8$ cm		$m_0 = 0.6\%$			$m_{P,0} = 3.0\%$		$\sigma_{\chi,0} = 1.5°$							
$\lambda = 0.9$ cm		$m_0 = 3.0\%$												
Source	N	I [Jy]	m [%]	χ^2_r	Y [%]	type	P [Jy]	m_P [%]	χ^2_r	Y_P [%]	χ [°]	m_χ [°]	χ^2_r	Y_χ [°]
0602+673	96	1.01	0.8	2.5	1.7	I	0							
	20	0.96	0.6	1.1		0	0.009	24.3	6.6	72.5	15.7	5.8	3.4	16.7
	19	0.68	4.1	1.8		0	–							
0716+714	96	1.04	2.7	25.6	7.7	I	0.055	10.6	41.7	31.3	10.8	1.9	5.5	5.2
	21	1.28	1.6	7.3	4.3	II	0.088	4.2	1.7		22.0	0.8	0.3	
	20	1.46	5.5	3.2	13.7	II	–							
0831+557	17	5.42	0.5	1.0		0	0							
	16	2.45	0.4	0.5		0	0							
	16	0.57	2.6	0.7		0	–							
0836+710	96	2.29	0.8	2.2	1.5	I	0.178	1.0	0.4		104.1	0.3	0.1	
	33	2.37	0.5	0.7		0	0.097	2.5	0.6		110.2	0.6	0.2	
	32	1.50	2.5	0.7		0	–							
0917+624	91	1.51	1.8	11.7	5.1	I	0.036	7.1	17.6	20.7	56.9	2.3	6.9	6.3
	21	1.41	0.9	2.6	2.1	II	0.026	8.5	4.3	24.0	70.1	4.3	6.1	12.0
	20	0.99	4.2	1.9		0	–							

Table 13. Observations from February 1999.

$\lambda = 6$ cm		$m_0 = 0.7\%$			$m_{P,0} = 3.0\%$		$\sigma_{\chi,0} = 2.0°$				$T = 6$ d			
Source	N	I [Jy]	m [%]	χ^2_r	Y [%]	type	P [Jy]	m_P [%]	χ^2_r	Y_P [%]	χ [°]	m_χ [°]	χ^2_r	Y_χ [°]
0716+714	20	0.95	5.1	52.0	15.1	I	0.028	17.2	73.4	50.7	22.7	3.1	2.4	7.2
0831+557	16	5.41	0.3	0.2		0	0							
0836+710	21	2.41	0.3	0.3		0	0.170	2.0	1.0		104.8	0.4	0.1	
0917+624	18	1.54	5.0	54.8	14.9	II	0.035	15.6	39.0	46.0	55.9	3.7	3.2	9.4
0954+658	17	0.30	1.3	3.8	3.5	II	0.009	24.2	84.7	71.9	−5.0	8.8	18.2	25.7

than the variability time-scale, brightness temperatures of up to 10^{17} K can be explained in this model with moderate Lorentz factors ($\Gamma \simeq 10-20$).

Coherent emission processes caused e.g. by the reconnection of magnetic field lines (e.g. Benford 1992; Lesch & Pohl 1992) could avoid the violation of the inverse Compton limit. At present, however, it is unclear whether this process can produce correlated broad band variations.

IDV could also be caused by extrinsic mechanisms, e.g. scattering in the interstellar medium (ISS, e.g. Rickett et al. 1995; Dennett-Thorpe & de Bruyn 2000; Rickett et al. 2001). The time-scale of variations, $\tau_{\rm var}$ caused by ISS depends on the scattering angle $\theta_{\rm scat}$, the distance to the scattering screen L, and the earth's velocity v relative to the screen: $\tau_{\rm var} \simeq (\theta_{\rm scat} \cdot L)/v$ (Rickett 1990). Typical values ($\theta_{\rm scat} \simeq 1$ mas, $L \simeq 500$ pc, $v \simeq 50\,{\rm km\,s^{-1}}$, e.g. Rickett 1990), result in a time scale of more than ten days. Hence, an explanation of IDV by ISS requires either a much closer scattering screen or a much higher velocity of the screen relatively to the earth. The presence of several distinct time-scales (as seen e.g. in 0716+714) makes this scenario even more complicated and indicates a stratified structure of the ISM. For 0917+624, an annual modulation in the scintillation time scale due to the earth's motion relative to the scattering screen was proposed by Rickett et al. (2001, see also Jauncey & Macquart 2001). However, subsequent observations could not confirm this behavior (Fuhrmann et al. 2002).

To explain the polarization angle variations, either a source consisting of multiple components or anisotropic scattering in an inhomogeneous medium has to be assumed. However, Qian et al. (2001) have shown that even a complex multi-component model was insufficient to fit the polarization variability satisfactorily.

Correlated broad-band variability would rule out ISS as the exclusive origin of IDV, since the variability strength should decrease with frequency. Nevertheless, even if IDV is a predominantly intrinsic phenomenon, it implies small source sizes and should therefore be accompanied by ISS.

To date, none of the models discussed above is fully capable of explaining all of the observed properties of IDV. It is therefore likely that the observed rapid variability is a complex superposition of source intrinsic and propagation effects.

Acknowledgements. This research is based on observations with the 100-m telescope of the MPIfR (Max-Planck-Institut für Radioastronomie) at Effelsberg. We are very grateful to the staff at the observatory for their support. We thank the referee, C. Fanti, and R.W. Porcas for critically reading the manuscript and valuable comments. This research has made use of the NASA/IPAC Extragalactic Database (NED) which is operated by the Jet Propulsion Laboratory, California Institute of Technology, under contract with the National Aeronautics and Space Administration.

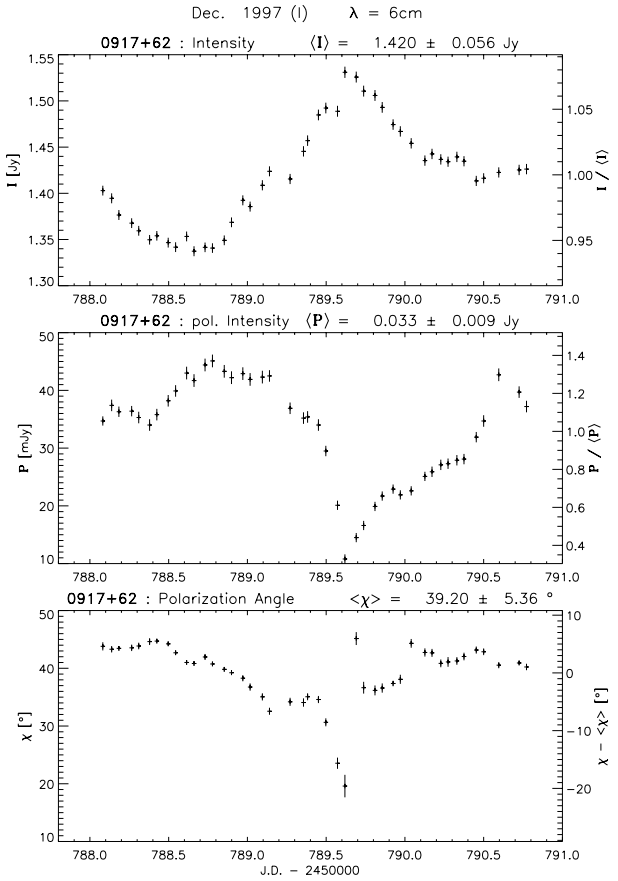

Fig. 5. Typical IDV in the quasar 0917+624 in December 1997. The variations in total intensity (top panel) are clearly anti-correlated with the polarized intensity (middle and bottom panel) changes (see also Fig. 6).

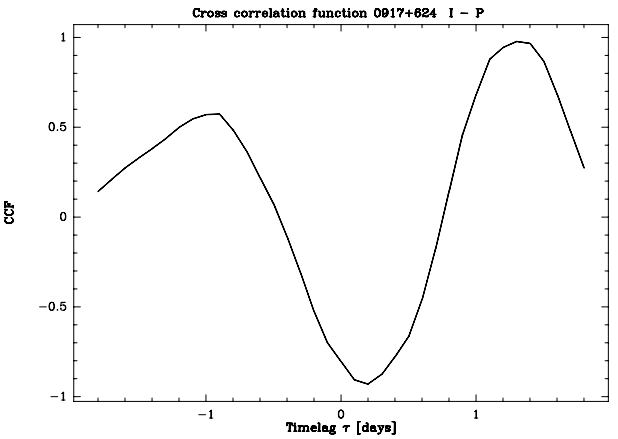

Fig. 6. Cross correlation function of the total and polarized intensity of 0917+624 in December 1997 (compare to Fig. 5 and text). This indicates a strong anti-correlation between the variability in total and polarized flux density.

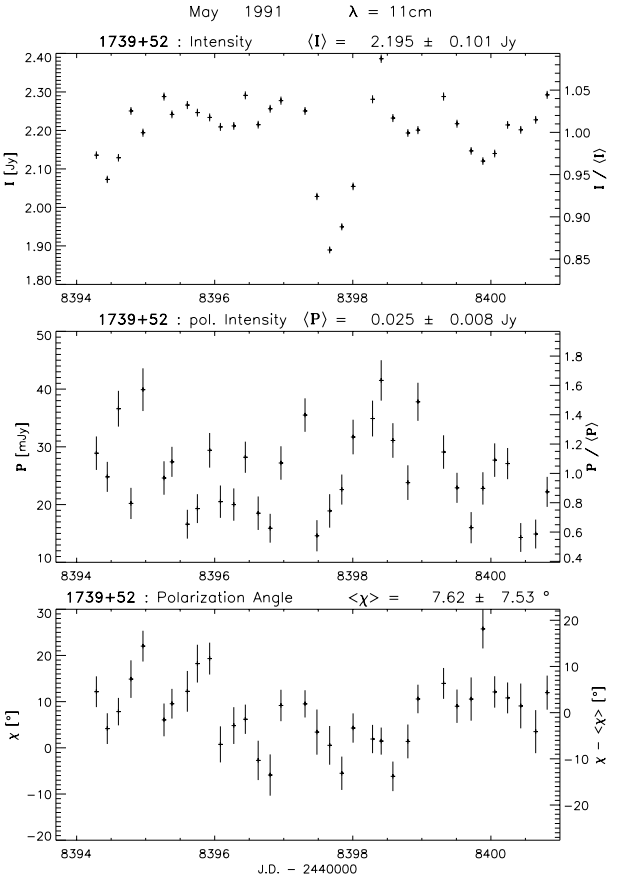

Fig. 7. Light curve of 1739+522 in May 1991. The fast dip of the total intensity is similar to an extreme scattering event, but much faster (see text).

References

Baars, J. W. M., Genzel, R., Pauliny-Toth, I. I. K., & Witzel, A. 1977, A&A, 61, 99

Begelman, M. C., Rees, M. J., & Sikora, M. 1994, ApJ, 429, L57

Benford, G. 1992, ApJ 391, L59

Bevington, P. R., & Robinson, D. K. 1992, Data reduction and error analysis for the physical sciences (New York: McGraw-Hill)

Blandford, R. D. 1990, in Saas-Fee Advanced Course 20, Active Galactic Nuclei, ed. R. D. Blandford, H. Netzer, & L. Woltjer (Springer), 161

Blandford, R. D., & Königl, A. 1979, ApJ, 232, 34

Britzen, S., Witzel, A., Krichbaum, T. P., et al. 2001, Astron. Lett., 27, 1

Cimò, G., Beckert, T., Krichbaum, T. P., et al. 2002, Publ. Astron. Soc. Aust., 19, 10

Dennett-Thorpe, J., & de Bruyn, A. G. 2000, ApJ, 529, L65

Edelson, R. A., & Krolik, J. H. 1988, ApJ, 333, 646

Fiedler, R. L., Dennison, B., Johnston, K. J., et al. 1994, ApJ, 430, 581

Fuhrmann, L., Krichbaum, T. P., Cimò, G., et al. 2002, Publ. Astron. Soc. Aust., 19, 64

Gabuzda, D. C., Kochenov, P. Yu., Kollgaard, R. I., & Cawthorne, T. V. 2000a, MNRAS, 315, 229

Gabuzda, D. C., Kochenov, P. Yu., & Cawthorne, T. V. 2000b, MNRAS, 319, 1125

Ghisellini, G., Padovani, P., Celotti, A., & Maraschi, L. 1993, ApJ, 407, 65

Heeschen, D. S., Krichbaum, T. P., Schalinski, C. J., & Witzel, A. 1987, AJ, 94, 1493

Heidt, J., & Wagner, S. J. 1996, A&A, 305, 42

Homan, D. C., Attridge, J. M., & Wardle, J. F. C. 2001, ApJ, 556, 113

Jauncey, D. L., & Macquart, J.-P. 2001, A&A, 370, L9

Jorstad, S. G., Marscher, A. P., Mattox, J. R., et al. 2001, ApJS, 134, 181

Kedziora-Chudczer, L. L., Jauncey, D. L., Wieringa, M. H., et al. 1997, ApJ, 490, L9
Kedziora-Chudczer, L. L., Jauncey, D. L., Wieringa, M. H., et al. 2001, MNRAS, 325, 1411
Kellermann, K. I., & Pauliny-Toth, I. I. K. 1969, ApJ, 155, L71
Kraus, A., Krichbaum, T. P., & Witzel, A. 1999a, in BL Lac phenomenon, ed. L. Takalo, & A. Sillanpää, ASP Conf. Ser., 159, 49
Kraus, A., Witzel, A., & Krichbaum, T. P. 1999b, New Astron. Rev., 43, 685
Kraus, A., Witzel, A., Krichbaum, T. P., et al. 1999c, A&A, 352, L107
Krichbaum, T. P., Quirrenbach, A., & Witzel, A. 1991, in Variability of Blazars, ed. E. Valtaoja, & M. Valtonen (Cambridge University Press), 331
Krichbaum, T. P., Kraus, A., Fuhrmann, L., et al. 2002, Publ. Astron. Soc. Aust., 19, 14
Kühr, H., Witzel, A., Pauliny-Toth, I. I. K., & Nauber, U. 1981, A&AS, 45, 367
Lesch, H., & Pohl, M. 1992, A&A, 254, 29
Lobanov, A. P., Krichbaum, T. P., Witzel, A., et al. 1998, A&A, 340, L60
Ott, M., Witzel, A., Quirrenbach, A., et al. 1994, A&A, 284, 331
Otterbein, K., Krichbaum, T. P., Kraus, A., et al. 1998, A&A, 334, 489
Peng, B., Kraus, A., Krichbaum, T. P., et al. 2000, A&A, 353, 937
Qian, S. J., Quirrenbach, A., Witzel, A., et al. 1991, A&A, 241, 15
Qian, S. J., Witzel, A., Kraus, A., et al. 1996, in Energy transport in radio galaxies and quasars, ed. P. Hardee, A. Bridle, & J. A. Zensus, ASP Conf. Ser., 100, 55
Qian, S. J., Witzel, A., Kraus, A., et al. 2001, A&A, 367, 770
Quirrenbach, A., Witzel, A., Qian, S. J., et al. 1989, A&A, 226, L1
Quirrenbach, A., Witzel, A., Wagner, S. J., et al. 1991, ApJ, 372, L71
Quirrenbach, A., Witzel, A., Krichbaum, T. P., et al. 1992, A&A, 258, 279
Quirrenbach, A., Kraus, A., Witzel, A., et al. 2000, A&AS, 141, 221 (Paper I)
Rickett, B. J. 1990, ARA&A, 28, 561
Rickett, B. J., Quirrenbach, A., Wegner, R., et al. 1995, A&A, 293, 479
Rickett, B. J., Witzel, A., Kraus, A., Krichbaum, T. P., & Qian, S. J. 2001, ApJ, 550, L11
Romero, G. E., Cellone, S. A., & Combi, J. A. 2000, A&A, 360, L47
Simonetti, J. H., Cordes, J. M., & Heeschen, D. S. 1985, ApJ, 296, 46
Spada, M., Salvati, M., & Pacini, F. 1999, ApJ, 511, 136
Stickel, M., Meisenheimer, K., & Kühr, H. 1994, A&AS, 105, 211
Turlo, Z., Forkert, T., Sieber, W., & Wilson, W. 1985, A&A, 142, 181
Wagner, S. J., & Witzel, A. 1995, ARA&A, 33, 163
Wagner, S. J., Witzel, A., Krichbaum, T. P., et al. 1993, A&A, 271, 344
Wegner, R. 1994, Ph.D. Thesis, University of Bonn
Weiler, K. W., & de Pater, I. 1983, ApJS, 52, 293
White, R. J., & Peterson, B. M. 1994, PASP, 106, 879
Witzel, A., Heeschen, D. S., Schalinski, C., & Krichbaum, T. P. 1986, Mitt. d. Astron. Gesell., 65, 239
Witzel, A., Schalinski, C. J., Johnston, K. J., et al. 1988, A&A, 206, 245